Organic & Biomolecular Chemistry

Dynamic Article Links

Cite this: *Org. Biomol. Chem.*, 2011, **9**, 5047

www.rsc.org/obc

COMMUNICATION

# Enantioselective binding of a lanthanide(III) complex to human serum albumin studied by $^1$H STD NMR techniques†

**David M. Dias,[a] João M. C. Teixeira,[a] Ilya Kuprov,[b] Elizabeth J. New,[b] David Parker[b] and Carlos F. G. C. Geraldes*[a]**

***Received 4th April 2011, Accepted 17th May 2011***
**DOI: 10.1039/c1ob05524k**



**The enantioselective binding of the (*SSS*)-Δ isomer of an yttrium(III) tetraazatriphenylene complex to 'drug-site II' of human serum albumin (HSA) was detected by the intensity differences of its STD $^1$H NMR spectrum relative to the (*RRR*)-Λ isomer, by the effect of the competitive binder to that site, *N*-dansyl sarcosine, upon the STD spectrum of each isomer, in the presence of HSA and by 3D docking simulations.**

Highly emissive complexes of the lanthanide(III) ions show great promise as chemosensors for potential application in studying biological systems.[1–9] Much current research focuses on the relationship of structure to various aspects of chemical and biological behaviour, in order to improve promising complexes and to design new complexes for specific purposes.[10–14]

In order for a lanthanide(III) complex to have potential utility as a biological probe, it must retain its selectivity and response in the cellular environment, notably in the presence of the high intracellular concentrations of proteins. Recent studies of potential luminescent lanthanide probes have investigated the effect of protein binding on their *in vitro* behaviour.[10,12,14–16] One such investigation yielded a novel example of dynamic helicity inversion following enantioselective protein binding: the (*SSS*)-Δ enantiomer of [Ln.**L**]$^{3+}$ (Scheme 1, Ln = Tb, Eu) binds to human serum albumin (HSA) with a resulting helicity change as measured by circularly polarised luminescence (CPL).[17] In contrast, the (*RRR*)-Λ enantiomer associates more weakly with the protein and does not exhibit this inversion. This behaviour was unique to the complex structure, and was not replicated by other complexes bearing either the same chromophore or pendant arms. Here, we report efforts to define the regions of the complex which bind to the protein by employing saturation transfer difference (STD) NMR techniques.

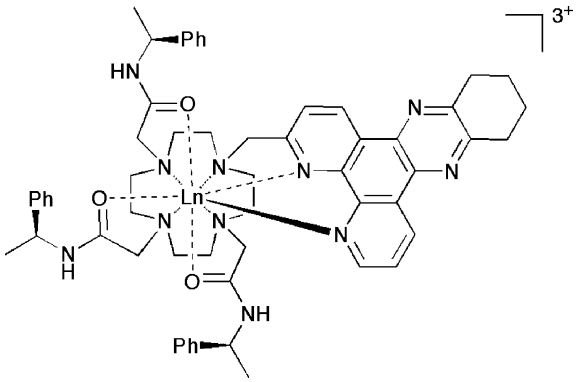


**Scheme 1** Chemical structure of the (*SSS*)-Δ enantiomer of [Ln.L]$^{3+}$ (Ln = Tb, Eu, Y).

STD NMR is commonly used to characterise the binding in ligand–receptor complexes.[18–21] In this method, selective irradiation of the protein NMR spectrum results in saturation of the protein signals and of any ligand protons interacting with the protein. Subtraction of this spectrum from the one collected in non-saturated protein and ligand conditions gives the saturation transfer difference spectrum, in which only protein-interacting protons are visible and the epitope is mapped by analysing the signal intensities of these protons in the STD spectrum.[19]

STD NMR requires the use of a diamagnetic metal ion, which precludes the direct study of Eu(III) or Tb(III) complexes. The diamagnetic yttrium(III) is a good model for Eu(III) and Tb(III), with an ionic radius that is only 0.02 Å smaller than Tb(III) in nine-coordinate systems.[22] Y(III) complexes were synthesized from the (*RRR*) and (*SSS*) isomers of **L** from yttrium acetate, using analogous procedures to those described previously for Eu(III), Tb(III) and Gd(III) complexes of **L**.[4]

While complete assignment of the $^1$H NMR spectra of **L** or [Eu.**L**]$^{3+}$ was hampered by exchange broadening associated with the conformational flexibility of the ligand and the broad peaks observed for the paramagnetic Eu(III) complex, the [Y.**L**]$^{3+}$ complexes were found to exist primarily as a single enantiomer in solution, giving rise to sharp NMR resonances. This enabled assignment of most protons in the complex from the well-defined COSY spectrum (Fig. S1, S2 in the ESI†). Two of the three phenyl amide pendant arms exhibit very similar chemical shifts, while resonances of the third lie about 1 ppm to lower frequency. This

[a]*Department of Life Sciences and Center of Neurosciences and Cell Biology, Faculty of Science and Technology, University of Coimbra, P.O. Box 3046, 3001-401 Coimbra, Portugal. E-mail: geraldes@bioq.uc.pt*
[b]*Department of Chemistry, Durham University, South Road, Durham, UK, DH1 3LE. E-mail: david.parker@durham.ac.uk*

† Electronic supplementary information (ESI) available: 600 MHz COSY NMR spectrum of (*SSS*)-Δ[Y.**L**]$^{3+}$ (Fig. S1) and 1D spectrum with partial assignments (Fig. S2); $^1$H STD NMR spectra of 30 μM HAS and 900 μM (*SSS*)-Δ[Y.**L**]$^{3+}$ (Fig. S3) or 900 μM (*RRR*)-Δ[Y.**L**]$^{3+}$ (Fig. S4) in the absence and in the presence of 2mM *N*-dansyl sarcosine. See DOI: 10.1039/c1ob05524k

**Table 1** STD amplification factor ($A_{STD}$) and relative STD (to the most shifted proton) for 900 μM (*SSS*)-Δ and (*RRR*)-Λ [Y.**L**]$^{3+}$ in the presence of 30 μM HSA, and changes in the relative STD for (*SSS*)-Δ and (*RRR*)-Λ [Y.**L**]$^{3+}$ upon addition of 2 mM *N*-dansyl sarcosine

| | (*RRR*)-Λ [Y.L]$^{3+}$ | | (*SSS*)-Δ [Y.L]$^{3+}$ | | | % change after *N*-dansyl-sarcosine | |
|---|---|---|---|---|---|---|---|
| Proton-ppm | $A_{STD}$ | Relative STD (%) | $A_{STD}$ | Relative STD (%) | % (*SSS*)–%(*RRR*) | (***RRR***)-Λ | (***SSS***)-Δ |
| 1′-9.6 | 3.51 | 100 | 4.08 | 100 | — | — | — |
| 3-9.5 | 2.50 | 71.2 | 3.86 | 94.6 | 23.4 | 8.8 | –30.5 |
| 3′-9.3 | 1.46 | 41.5 | 2.41 | 59.0 | 17.5 | 12.0 | –36.8 |
| 2′-8.35 | 2.63 | 75.0 | 3.24 | 79.5 | 4.5 | 23.9 | 24.7 |
| f-7.04 | 1.88 | 53.6 | 3.19 | 78.1 | 24.5 | 0.5 | –62.8 |
| 2(e.d)-6.4 | 2.48 | 70.8 | 3.75 | 91.8 | 21.1 | 15.4 | –37.7 |
| 4.4′-3.2 | 1.65 | 47.1 | 2.67 | 65.4 | 18.2 | –16.5 | –41.1 |
| 5.5′-2.0 | 1.74 | 49.6 | 2.86 | 70.0 | 18.5 | –13.1 | –33.8 |
| Me.2-1.6 | 0.62 | 17.6 | 1.03 | 25.2 | 7.6 | –4.9 | –14.6 |
| Me.1-1.1 | 1.34 | 38.2 | 2.07 | 50.8 | 12.5 | –10.8 | –30.6 |
| Me.3-0.8 | 1.21 | 34.6 | 2.11 | 51.7 | 17.1 | –0.5 | –15.9 |

shift is consistent with a deshielding ring current effect associated with a through-space interaction involving another aromatic system. The molecular geometry of the two isomers of [Y.**L**]$^{3+}$ was calculated using density function theory (DFT), which indicated that one of the pendant arms adjacent to the chromophore lies directly above the aromatic portion of the chromophore, giving rise to this deshielding effect (Fig. 1).

Following assignment of the [Y.**L**]$^{3+}$ spectrum, STD NMR spectra were acquired for the two enantiomers in the presence of HSA, with pre-saturation of the protein at –0.5 ppm (Fig. 2). The two complexes were compared by calculation of the STD amplification factors, $A_{STD}$, the relative intensity of the STD signal compared to that of the most shifted ligand proton (Table 1). The $A_{STD}$ values for all measured protons of the (*SSS*)-Δ isomer are larger than for the corresponding protons of the (*RRR*)-Λ; for almost every proton, the difference between the two isomers is greater than 10%. Given the HSA binding isotherm for the (*SSS*)-Δ isomer (log$K$ = 5.1 for a 1 : 1 binding model) and the observed multi-site binding of the (*RRR*)-Λ isomer consistent with stepwise formation of various adducts of lower affinity,[17] we attribute the higher $A_{STD}$ values of the (*SSS*)-Δ isomer protons to its stronger protein interaction, as found previously.[17]

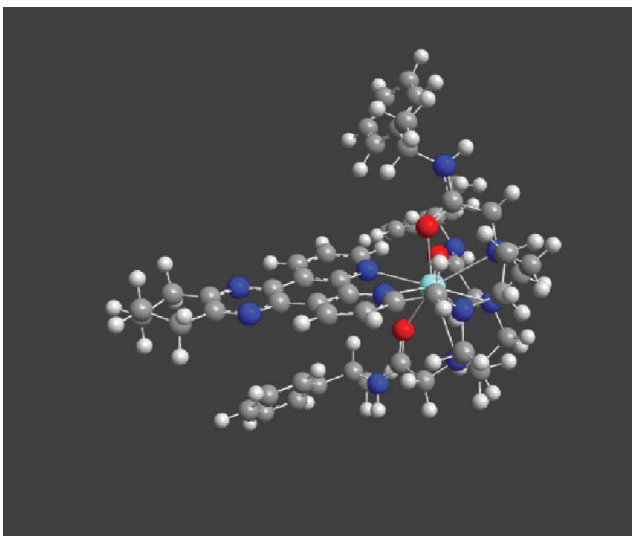

**Fig. 1** Molecular geometry of (*SSS*)-Δ [Y.**L**]$^{3+}$ optimized in Gaussian03 using DFT with PBE exchange-correlation functional, cc-pVDZ basis set on the light atoms and Stuttgart RSC 1997 ECP basis set on yttrium.

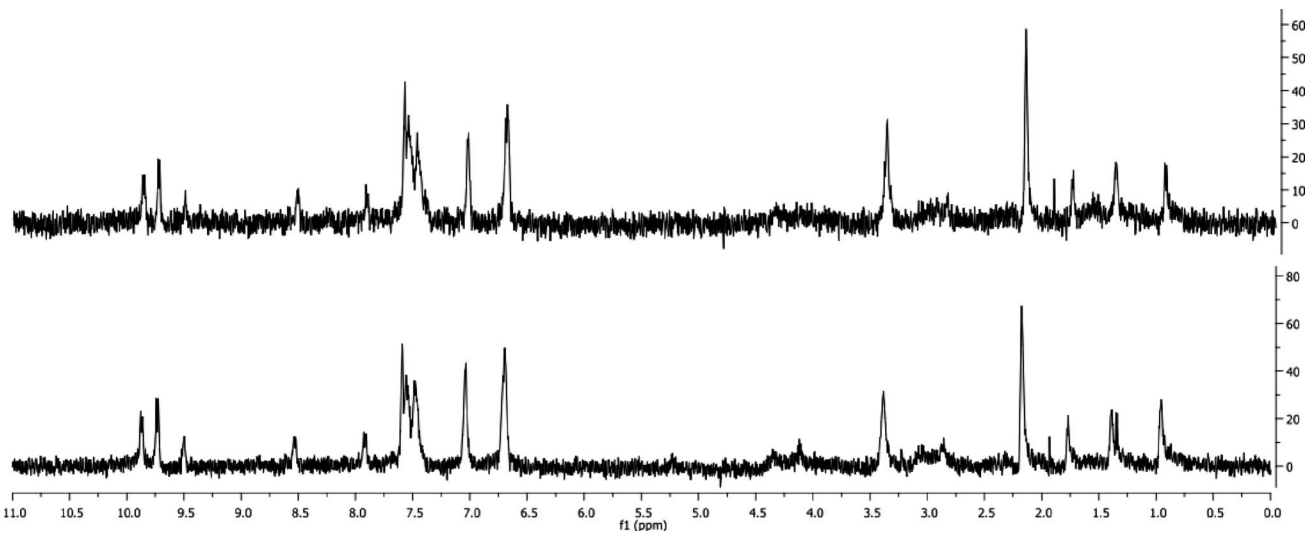


**Fig. 2** $^1$H STD NMR of (*SSS*)-Δ (upper) and (*RRR*)-Λ [Y.**L**]$^{3+}$ (lower) in the presence of 30 μM HSA (1 mM complex, 25 °C, $D_2O$, 600 MHz, –0.5 ppm saturation).

 

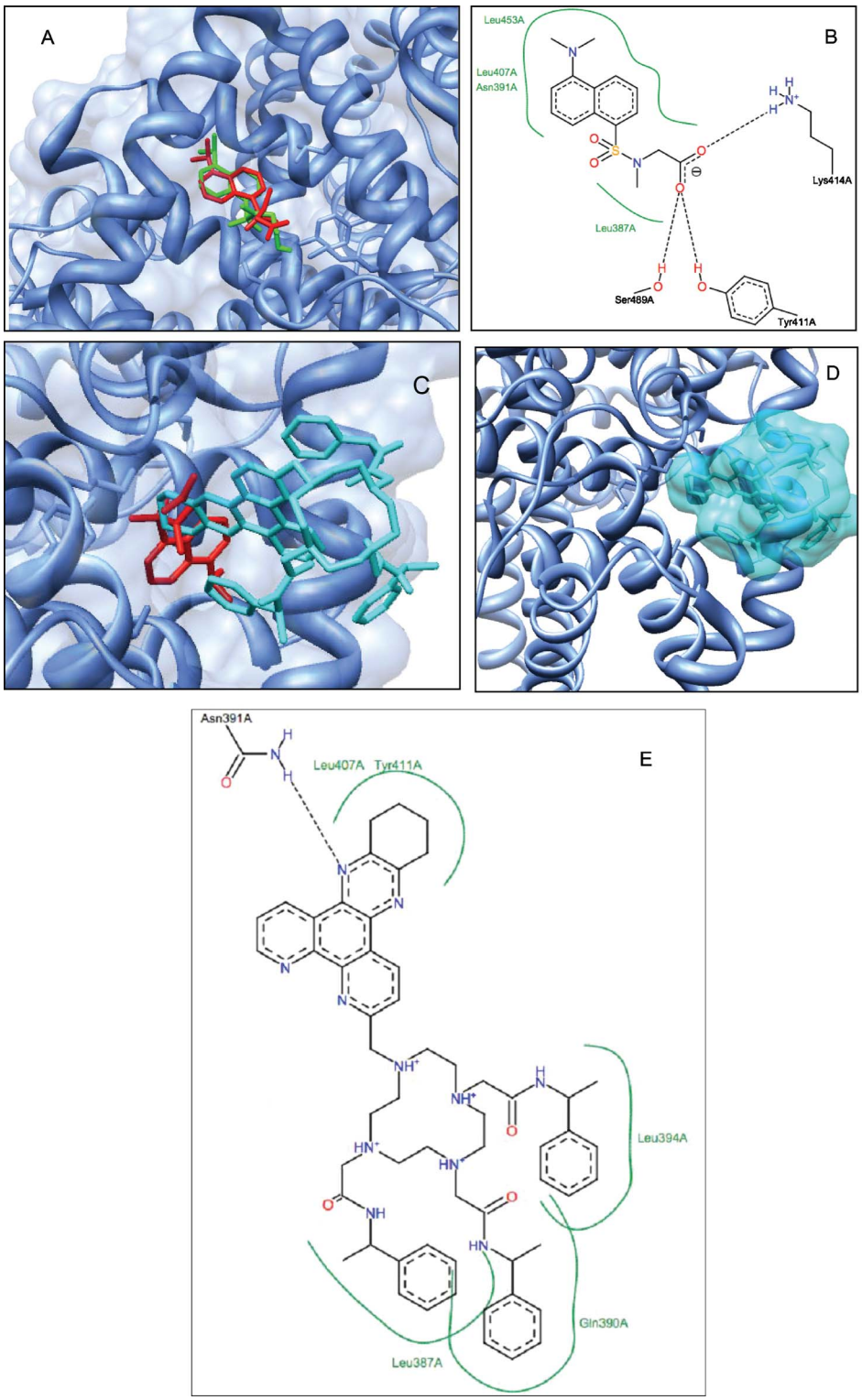


**Fig. 3** (A) *N*-dansyl sarcosine, a known binder of HSA drug site II. Overlay of structures from X-ray structure 2XVQ.pdb (red) and docked with Autodock Vina (green); (B) 2D scheme for interactions between *N*-dansyl sarcosine and site II of HSA, (black dashed lines—hydrogen bonds; green solid lines—hydrophobic interactions); (C and D) docked structure for (*SSS*)-Δ isomer (cyan) overlaid with and without *N*-dansyl sarcosine (red), respectively, indicating a specific competition for this site and a lodging inside the binding site. (E) 2D scheme for interactions between (*SSS*)-Δ isomer and site II of HSA (black dashed lines—hydrogen bonds, green solid lines—hydrophobic interactions, green dashed lines—Pi-cation interactions).

Analysis of the STD NMR spectrum of (*SSS*)-[Y.**L**]$^{3+}$ allows identification of the region of the complex that interacts with the protein. The protons that appear in the standard NMR spectrum, but not in the STD spectrum, correspond to the cyclen ring and the amide methylene groups, which do not interact with the protein, consistent with their location in the centre of the complex, shielded by the pendant arms and chromophore. In addition, protons from the pendant arm that interacts with the chromophore and the cyclohexyl ring of the chromophore do not appear in the STD spectrum, or have very similar $A_{STD}$ values to the (*RRR*)-Λ enantiomer, indicating that this moiety is not in the main core of the interaction with HSA.

Previously-reported proton relaxometric studies of the corresponding Gd(III) complex demonstrated the selectivity of binding of the complex to drug site II of HSA, identified by competition assays with the site-selective ligand *N*-dansyl sarcosine.[17] This interaction was also studied by an STD NMR experiment, in which *N*-dansyl sarcosine was added to the mixtures of protein and complex (Fig. S3 and S4 in the ESI†). STD amplification factors for the (*SSS*)-Δ isomer in the presence of *N*-dansyl sarcosine are vastly different from those measured in the absence of the competitor, while there is less difference for the (*RRR*)-Λ enantiomer (Table 1). These results corroborate the findings of the relaxivity studies.[17]

Since the X-ray structure of *N*-dansyl sarcosine-bound HSA is available, a molecular docking simulation of the interaction of HSA binding site II with the most interacting (*SSS*)-Δ enantiomer was performed using Autodock Vina[23] in order to provide a 3D model of the interaction. Among the population of possible orientations for the ligand at the HSA binding site, the one with the lowest docked energy was selected (Fig. 3). This software, however, does not support yttrium, and thus it was removed, remaining its structurally unchanged cage. Since, due to this limitation, three units of positive charge and its subsequent energy interaction are lost, these simulations are considered a qualitative three-dimensional search and not a quantitative model. The simulated 3D orientation of *N*-dansyl sarcosine at the HSA binding site II and the 2D interaction model coincide with the X-ray structure (Fig. 3A,B). The 3D scheme (Fig. 3C,D) shows that the (*SSS*)-Δ isomer interacts directly with the drug site II, mainly through the phenylmethyl pendant arms and the aromatic region of the chromophore, as suggested by the STD NMR data. This provides an explanation for the observation that this binding behaviour requires conservation of both the chromophore structure and the pendant arms. A 2D model (Fig. 3E) was also established based on the docking results and using Poseview,[24,25] which highlights the direct competition of the complex with *N*-dansyl sarcosine for interaction with the same residues, mainly Tyr 411, Asn 391 and Leu 387. This 2D view depicts the hydrophobic contact of the phenylmethyl pendant arms and the chromophore with HSA, which is further stabilized by an hydrogen bond between Asn 391 and a chromophore nitrogen.

In summary, this work has demonstrated the utility of STD NMR experiments in providing detailed structural information about the protein binding interaction. The study confirms that (*SSS*)-Δ [Ln.**L**]$^{3+}$ associates selectively with HSA compared to the (*RRR*)-Λ enantiomer, and identifies the regions of the complex which directly interact with drug site II of the protein.

We thank the Association of Commonwealth Universities (EJN), the Fundação para a Ciência e Tecnologia (FCT), Portugal (project PTDC/QUI/70063/2006) FEDER and ESF-COST D38 for support. The Varian VNMRS 600 NMR spectrometer in Coimbra was acquired with the support of the FCT Programa Nacional de Reequipamento Científico, contract REDE/1517/RMN/2005, as part of RNRMN (Rede Nacional de RMN).

## Notes and references

1 Y. Bretonniere, M. J. Cann, D. Parker and R. Slater, *Chem. Commun.*, 2002, 1930–1931.
2 J.-C. G. Bünzli, in *Metal Ions in Biological Systems-The Lanthanides and Their Interrelations with Biosystems*A. Sigel, H. Sigel, ed.; Marcel Dekker: New York, 2003.
3 K. Hanaoka, K. Kikuchi, H. Kojima, Y. Urano and T. J. Nagano, *J. Am. Chem. Soc.*, 2004, **126**, 12470–12476.
4 R. A. Poole, G. Bobba, M. J. Cann, J.-C. Frias, D. Parker and R. D. Peacock, *Org. Biomol. Chem.*, 2005, **3**, 1013–1024.
5 S. Pandya, J. Yu and D. Parker, *Dalton Trans.*, 2006, 2757–2766.
6 J. Yu, D. Parker, R. Pal, R. A. Poole and M. J. Cann, *J. Am. Chem. Soc.*, 2006, **128**, 2294–2299.
7 C. D. Vandevyver, A. S. Chauvin, S. Comby and J.-C. G. Bünzli, *Chem. Commun.*, 2007, 1716–1718.
8 C. P. Montgomery, B. S. Murray, E. J. New, R. Pal and D. Parker, *Acc. Chem. Res.*, 2009, **42**, 925–937.
9 E. J. New, D. Parker, D. G. Smith and J. W. Walton, *Curr. Opin. Chem. Biol.*, 2010, **14**, 238–246.
10 R. A. Poole, C. P. Montgomery, E. J. New, A. Congreve, D. Parker and M. Botta, *Org. Biomol. Chem.*, 2007, **5**, 2055–2062.
11 F. Kielar, G.-L. Law, E. J. New and D. Parker, *Org. Biomol. Chem.*, 2008, **6**, 2256–2258.
12 B. S. Murray, E. J. New, R. Pal and D. Parker, *Org. Biomol. Chem.*, 2008, **6**, 2085–2094.
13 E. J. New and D. Parker, *Org. Biomol. Chem.*, 2009, **7**, 851–855.
14 E. J. New, D. Parker and R. D. Peacock, *Dalton Trans.*, 2009, 672–679.
15 R. Pal, D. Parker and L. C. Costello, *Org. Biomol. Chem.*, 2009, **7**, 1525–1528.
16 C. P. Montgomery, E. J. New, L. O. Palsson, D. Parker, A. S. Batsanov and L. Lamarque, *Helv. Chim. Acta*, 2009, **92**, 2186–2213.
17 C. P. Montgomery, E. J. New, D. Parker and R. D. Peacock, *Chem. Commun.*, 2008, 4261–4263.
18 M. Mayer and B. Meyer, *Angew. Chem., Int. Ed.*, 1999, **38**, 1784–1788.
19 M. Mayer and B. Meyer, *J. Am. Chem. Soc.*, 2001, **123**, 6108–6117.
20 B. Meyer and T. Peters, *Angew. Chem., Int. Ed.*, 2003, **42**, 864–890.
21 J. Angulo, P. M. Enríquez-Navas and P. M. Nieto, *Chem.–Eur. J.*, 2010, **16**, 7803–7812.
22 R. D. Shannon, *Acta Crystallogr., Sect. A: Cryst. Phys., Diffr., Theor. Gen. Crystallogr.*, 1976, **32**, 751–767.
23 O. Trott and A. J. Olson, *J. Comput. Chem.*, 2010, **31**, 455–461.
24 K. Stierand, P. C. Maass and M. Rarey, *Bioinformatics*, 2006, **22**, 1710–1716.
25 K. Stierand and M. Rarey, *ChemMedChem*, 2007, **2**, 853–860.

 